Effects of Inhibitors on Hsp90′s Conformational Dynamics, Cochaperone and Client Interactions

Schmid, Sonja; Götz, Markus; Hugel, Thorsten

DOI
10.1002/cphc.201800342

Publication date
2018

Document Version
Final published version

Published in
ChemPhysChem

ChemPubSoc Europe

DOI: 10.1002/cphc.201800342

CHEMPHYSCHEM Articles

Effects of Inhibitors on Hsp90's Conformational Dynamics, Cochaperone and Client Interactions

Sonja Schmid,*[a, b] Markus Götz,[a, c] and Thorsten Hugel*[a]

The molecular chaperone and heat-shock protein Hsp90 has become a central target in anti-cancer therapy. Nevertheless, the effect of Hsp90 inhibition is still not understood at the molecular level, preventing a truly rational drug design. Here we report on the effect of the most prominent drug candidates, namely, radicicol, geldanamycin, derivatives of purine, and novobiocin, on Hsp90's characteristic conformational dynamics and the binding of three interaction partners. Unexpectedly, the global opening and closing transitions are hardly affected by Hsp90 inhibitors. Moreover, we find no significant changes in the binding of the cochaperones Aha1 and p23 nor of the model substrate Δ131Δ. This holds true for competitive and allosteric inhibitors. Therefore, direct inhibition mechanisms affecting only one molecular interaction are unlikely. We suggest that the inhibitory action observed in vivo is caused by a combination of subtle effects, which can be used in the search for novel Hsp90 inhibition mechanisms.

1. Introduction

The molecular chaperone and heat-shock protein Hsp90 is a metabolic hub.[1] It is involved in all *Six Hallmarks of Cancer*.[2] Due to this exceptional role, Hsp90 has become a central target in a broad range of anti-cancer therapies. Numerous studies have been undertaken, both by academia and industry, to develop Hsp90 inhibition strategies.[3] Nevertheless, the molecular basis of the observed therapeutic effects is still unknown, although it is essential for rational drug design. Mainly four classes of Hsp90 inhibitors have been investigated as anti-cancer drug candidates so far. Three of them bind to Hsp90's unusual, N-terminal ATP binding site, a rare Bergerat fold.[4] These are derivatives of geldanamycin[5], radicicol[6,7] and purine (e.g. PU–H71[8]). They are competitive inhibitors, which suggests ATPase inhibition as the mechanism. In addition, there is an allosteric inhibitor class: the novobiocin derivatives, sometimes called novologues[9,10] (e.g. KU-32),[11] which targets Hsp90's C-terminal domain. While the class of purine derivatives originates from *in silico* studies,[8,12] all the other main classes are natural product derivatives found by screening.[7] Although *in vivo* studies report measurable effects of these inhibitors, there is currently little *molecular* understanding of the inhibition mechanism of these drug candidates.

It is generally accepted that any mechanistic hypothesis must stand both, *in vivo* and *in vitro* testing. In an attempt to provide a better *molecular* understanding of anti-cancer drug candidates targeting Hsp90, and to complement the existing *in vivo* results, we report how well-known small molecular inhibitors affect important molecular observables in Hsp90's functional cycle *in vitro*.

First we probe the characteristic conformational changes between a v-shaped open conformation with dissociated N-domains, and a compact closed conformation where the three domains (N-terminal, middle, C-terminal) of the homodimer form inter-monomer contacts with their equivalent counterparts.[13–15] It is commonly assumed that these characteristic conformational changes are rate-limiting for Hsp90's function, involving ATP hydrolysis, cochaperone interaction and finally client processing.[16–18] Product release (ADP, P_i) was found not to be rate-limiting for ATP hydrolysis.[19]

We use single molecule Förster resonance energy transfer (smFRET), which is perfectly suited to reveal conformational dynamics that are usually hidden by ensemble averaging.[20,21] We attach one donor and one acceptor dye to specific residues of either Hsp90 monomer (Figure 1). The sensitivity of FRET on inter-dye distance changes enables us to distinguish open and closed conformations of Hsp90 and it allows us to record conformational changes in real-time with a total internal reflection fluorescence microscope (TIRFM). We provide a quantitative description of these kinetics, which became available by our recently developed single molecule analysis of complex kinetic sequences (SMACKS).[22] Altogether, this single molecule approach is very sensitive to drug induced changes in the relative population of open and closed conformations, and also to changes in transition kinetics between those.

Second, we investigate the *in vitro* effect of the inhibitors on the binding of two well characterized cochaperones, namely p23[23] and Aha1[24] using fluorescence anisotropy.

Third, we examine a possible interference of the inhibitors with substrate binding: the established model client Δ131Δ[25]

[a] *Dr. S. Schmid, Dr. M. Götz, Prof. Dr. T. Hugel*
Institute of Physical Chemistry, University of Freiburg, Albertstr. 23a, 79104 Freiburg (Germany)
E-mail: th@pc.uni-freiburg.de
s.schmid@tudelft.nl

[b] *Dr. S. Schmid*
present address: Department of Bionanoscience, Kavli Institute of Nanoscience Delft, Delft University of Technology, Van der Maasweg 9, 2629 HZ Delft (The Netherlands)

[c] *Dr. M. Götz*
present address: Centre de Biochimie Structurale, CNRS, Rue Serge Reggiani, 34090 Montpellier (France)

Supporting information for this article is available on the WWW under https://doi.org/10.1002/cphc.201800342

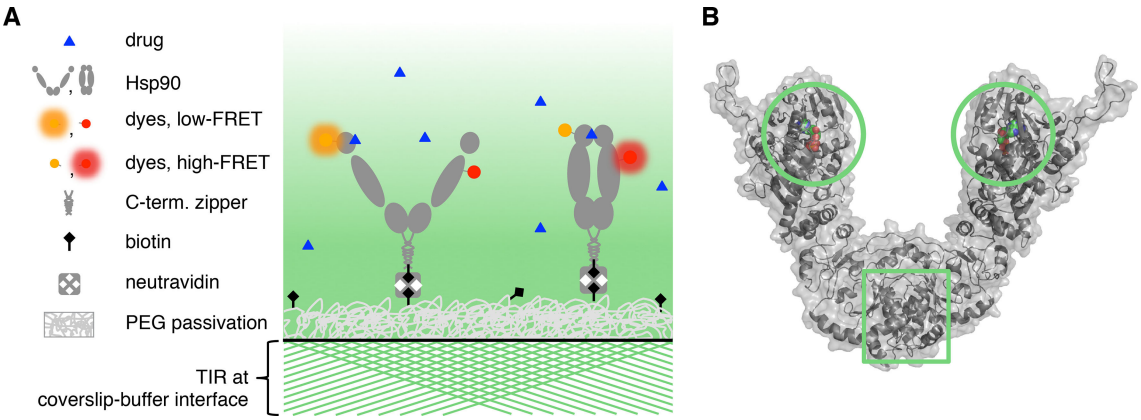

Figure 1. A) Illustration of the smFRET experiment revealing the effect of drug candidates on Hsp90's conformational dynamics. Single molecule FRET between the attached fluorescent dyes allows us to distinguish open and closed conformations of Hsp90. To follow one molecule for minutes, the dimers are stabilized by a C-terminal zipper motif (see Experimental Section) and immobilized on a polyethylene glycol (PEG) passivated coverslip using biotin-neutravidin coupling. Fluorescence intensities of individual dyes are recorded by total internal reflection (TIR) fluorescence microscopy. Schematic laser rays are depicted as green lines. The evanescent excitation intensity is shown in fading green. See example data in Figure 2A
B) Solution structure of the open conformation of Hsp90[14] in gray with nucleotides as colored spheres. The binding sites of the competitive (green circles), and C-terminal Novobiocin-derived inhibitors[10] (green square) are indicated.

binds between the M-domains of the Hsp90 dimer,[18] which is representative for many other clients.

Altogether we find that there is not a single straightforward inhibition mechanism for any of the major Hsp90 inhibitor classes, indicating that they might rather act on diverse features of the highly dynamic chaperone system.

2. Results

This study includes one lead compound of each main class of Hsp90 inhibitors, namely geldanamycin, radicicol, the purine derivative PU–H71[8,26] and novobiocin inspired KU-32[11] at saturating concentrations (see Experimental Section). The former three competitively inhibit Hsp90's ATPase function, whereas KU32 does not interfere with ATP hydrolysis (Supplementary Figure S1) nor AMP-PNP induced conformational closing (Supplementary Figure S2). Figure 2A shows example fluorescence traces obtained from individual fluorescently labeled Hsp90 dimers in the presence of one of these inhibitors, respectively. Specific conformational transitions are observed as an anti-correlated change in donor and acceptor fluorescence. In the closed conformation of Hsp90, both dyes are close to each other (approx. 53 Å) leading to high acceptor fluorescence and low donor fluorescence, due to efficient FRET. The opposite is the case in the open conformation, where the dyes are further apart (approx. 92 Å), causing low acceptor fluorescence and high donor fluorescence. The information from a total of over 600 molecules is combined in the FRET efficiency histograms in Figure 2B. We have previously shown that yeast Hsp90's prevalent conformation – under many conditions including saturating ADP as well as ATP – is an open, v-shaped one,[14] leading to low FRET efficiencies in the described smFRET experiment. In contrast, in the presence of the non-hydrolysable ATP analogue AMP-PNP, Hsp90 occurs mainly in the globally closed conformation (cf. crystal structure 2cg9)[13].

Interestingly, Figure 2B shows that clearly none of the four lead compounds provoked a shift similar to AMP-PNP. While individual example traces (Figure 2A) show some statistical variation, neither the competitive inhibitors nor the allosteric KU-32 changed the equilibrium distribution considerably. Therefore, a systematic shift in the conformational equilibrium directly caused by the inhibitors is most unlikely to cause the inhibitory effects observed *in vivo*. Obviously, identical equilibrium distributions can be caused by multiple sets of kinetic rate constants, i.e. the conformational *kinetics* could still vary. Therefore, we analyzed the observed kinetics more thoroughly using the software SMACKS.[22]

As shown in Figure 3A, a 4-state model with 3 links was found for Hsp90 in the presence of each of the four inhibitors, no matter from which class they were. The states 0/1 represent open conformations; states 2/3 denote closed conformations. Globally open or globally closed conformations may differ in local structural arrangements. Although not all four conformations are directly distinguishable in terms of FRET efficiency, the observed kinetic behavior implies a 4-state model:[22] in excellent agreement, this is shown by the dwell-time distributions and the Bayesian information criterion (Supplementary Figures S4 and S5). We generally observe the fastest transition rates between the short-lived states 1 and 2, whereas states 0 and 3 represent longer-lived but less frequently accessed states. For either inhibitor, state 0 is most populated followed by state 3, 1 and 2. The corresponding quantitative rate constants are displayed in Figure 3B. The uncertainty of the rate constants is reported as their 95% confidence interval. In the presence of AMP-PNP all transition rates differ significantly from the ADP case. The decreased opening and increased closing rate constants perfectly explain the drastic shift in the FRET histogram upon the addition of AMP-PNP in Figure 2B. In contrast, the effect induced by the inhibitors is small: while some significant differences are observed, these lie only marginally outside the confidence interval. There is also no systematic

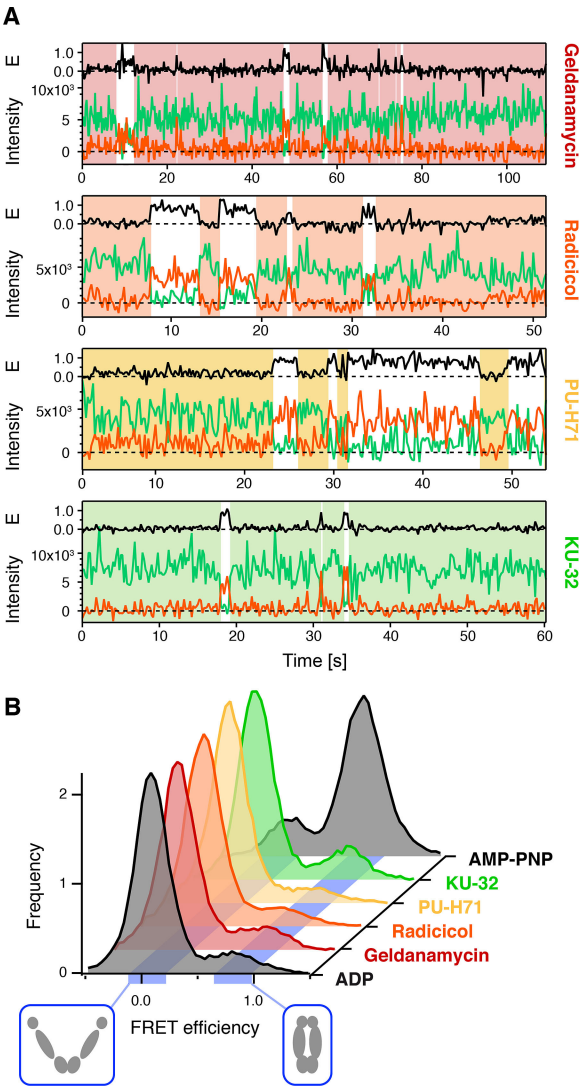

Figure 2. A) smFRET trajectories show conformational dynamics in the presence of the indicated inhibitor. Fluorescence intensities of individual FRET donor and acceptor dyes coupled to Hsp90 are shown as green and orange lines, respectively. The resulting FRET efficiency (E) is shown in black. Hsp90's closed and open conformations are indicated as white and colored overlays, respectively, given by the Viterbi path.[22] B) FRET histograms (normalized to unity) show that open conformations (low FRET) prevail under all conditions, except for the non-hydrolysable nucleotide analogue AMP-PNP, which stabilizes the closed conformation. Blue ribbons highlight the expected FRET efficiencies of the indicated open and closed conformations. n(ADP) = 107, n(geldanamycin) = 108, n(radicicol) = 142, n(PU–H71) = 123, n(KU-32) = 65, n(AMP-PNP) = 104. On average, the traces were 150–200 frames long, corresponding to 40 seconds. For clarity we omitted the directly excited acceptor trace. It can be found in Supplementary Figure S3, along with an AMP-PNP example trace.

difference between the N- and C-terminal inhibitors. Altogether, the observed small effects of the inhibitors on Hsp90's global conformational changes, cannot on their own explain the inhibitory effects found *in vivo*.

Next we investigate the effect of the inhibitors on Hsp90's interaction with cochaperones and a model client. Figure 4 shows the fluorescence anisotropy of the binding partners in absence and presence of the inhibitors. 10 μM Hsp90 and saturating amounts of the inhibitors were added to 200 nM Aha1 (fluorescently labeled at position 85), 400 nM p23 (labeled at position 2) or 400 nM Δ131Δ (labeled at position 16). As a control 2% (vol:vol) DMSO was added. The cochaperone and client concentrations were chosen to be below their respective K_d to reduce the fraction of unbound, labeled molecules, and therefore achieve maximal sensitivity. As the binding is not saturated, any change in the binding affinity upon addition of inhibitor can be detected sensitively. A significant increase of the anisotropy signal of the labeled species is observed when Hsp90 is present for all tested proteins, confirming binding. In contrast, in every single case the DMSO control shows larger or similar effects compared to the inhibitor. Therefore, it is unlikely that impaired binding of Hsp90 to these cochaperones or the client is the reason for the inhibitory effects found *in vivo*. Again, this holds for N- and C-terminal inhibitors. Note that the binding sites for these three investigated binding partners are at complementary positions. Aha1 and p23 mainly bind the closed state of Hsp90 at the N and M domains, while Δ131Δ binds mainly the open state in between the M domains.

3. Discussion

To date, the success of Hsp90 inhibitors in clinical trials has been moderate. One reason for this is the lack of a molecular understanding of their precise inhibitory action, preventing a rational drug design. Therefore, we undertook an *in vitro* study covering all four major classes of Hsp90 inhibitors, namely geldanamycin, radicicol and derivatives of purine and novobiocin. We first determined the complete *in vitro* kinetics of Hsp90's global opening/closing transitions under these inhibitor conditions. Interestingly, our results show that the characteristic transitions between globally open and closed conformations are hardly affected, although they are commonly believed to be rate-limiting for Hsp90's activity.[27] The observed alterations are neither systematic, nor strong, compared to the effect of AMP-PNP. Thus, it is very unlikely that a direct interference with these conformational changes represents the dominating inhibition mechanism. Similarly, weak effects are found for the interaction with typical cochaperones and a well-characterized model substrate. Therefore, an exclusive interference with one of these interactions is not a likely inhibition mechanism, either.

In addition, our findings help clarify some open points concerning Hsp90's working principle and inhibition mechanism. First, Hsp90's ATPase function is still controversially discussed.[16,18,28] A direct coupling of Hsp90's characteristic conformational changes to ATP hydrolysis is repeatedly proposed, despite contradicting evidence. If such a direct coupling was the case, competitive ATPase inhibition should ultimately abolish Hsp90's characteristic conformational changes. On the contrary, the presented results clearly show that such a causality must be dismissed, which supports earlier evidence[21] indicating that Hsp90's characteristic conformational dynamics do not rely on ATPase function. However, it is important to note here that the opposite conclusion does not necessarily hold. I.e. it is still possible that those dynamics are themselves rate-

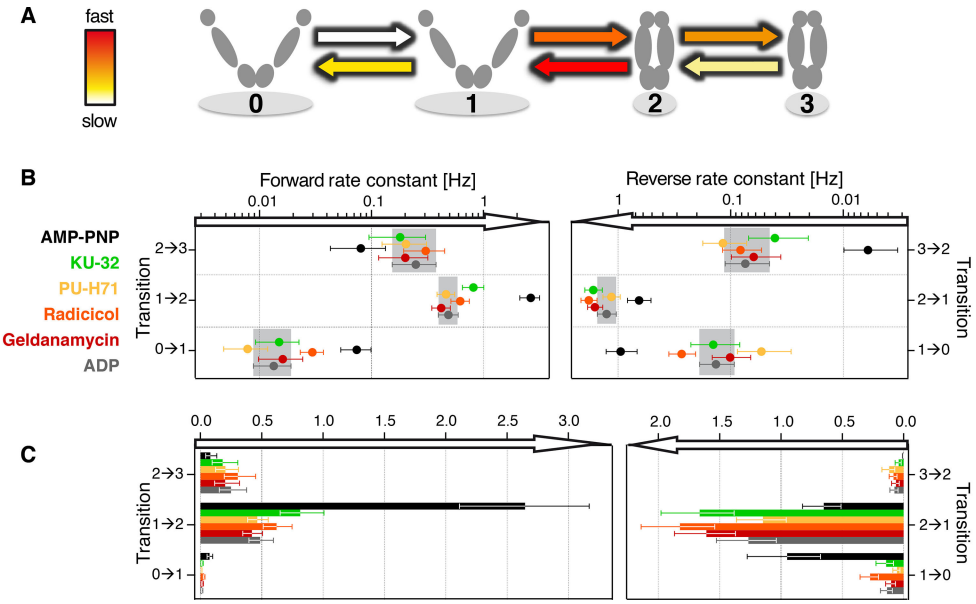

Figure 3. Kinetic model of Hsp90's conformational dynamics. A) Schematic consensus model under all tested inhibitor conditions, as well as ADP. B) Quantitative rate constants and confidence intervals of the transitions in (A). Gray areas represent the 95% confidence intervals in the presence of ADP. Significantly different rate constants were found with AMP-PNP (black), but none of the inhibitors changed the kinetics in a similar way. C) Same data as in (B) plotted in a linear scale.

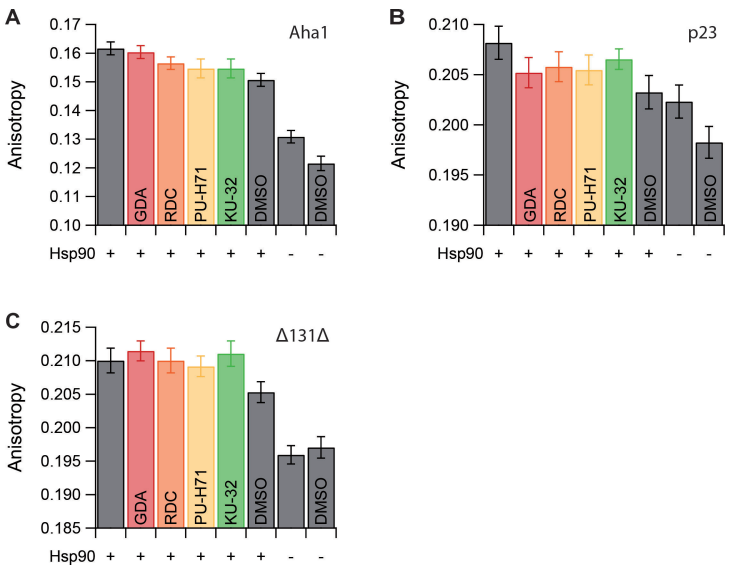

Figure 4. Hsp90 inhibitors show no significant effect on the binding of the cochaperones Aha1 and p23 or the model client Δ131Δ in fluorescence anisotropy experiments. The fluorescence anisotropy of labeled: A) Aha1, B) p23, or C) Δ131Δ is shown in absence or presence of the indicated inhibitor, or DMSO as a control. Error bars are the SD of the 31 data points that were taken for each sample.

limiting for the slow ATPase rate, although being independent of ATP hydrolysis themselves. Second, novobiocin derived inhibitors bind to the C-terminal domain, which represents the global hinge of the Hsp90 dimer. Therefore, effects on the large conformational dynamics were initially expected, but not observed in any of our experiments. Further discussed mechanisms of novobiocin derivatives include interference with client[29] and/or cochaperone (namely p23) interaction.[10,30] None of these proposed mechanisms withstood our *in vitro* testing.

We like to stress that, although *in vitro* experiments clearly fail to mimic the complex cellular conditions, they remain a valid and crucial hypothesis test. If any of the investigated interactions or conformational changes were directly affected by the inhibitors, it would be detectable *in vitro,* too.

Altogether our findings point towards a combination of small interferences, which jointly lead to the observed inhibitory effects. Such combined effects, e.g. on clients and cochaperones, are difficult to capture in any experiments, because they occur simultaneously and hence they are

undetectable in ensemble experiments. In addition, Hsp90's low-affinity interactions make single molecule experiments, similar to the ones described here, with multiple interaction partners very difficult. As a result, at the moment no reliable *in vitro* test exists to assess the potency of Hsp90 drug candidates, as neither ATPase activity, nor conformational changes, nor binding of the tested interaction partners are capable to predict the *in vivo* effect. Nevertheless, our results are the basis for future single molecule experiments in yeast lysate or even live human cell lines to possibly test the potency of drug candidates. We anticipate that our results also help in moving from sheer trial and error to biomedical comprehension of Hsp90's diverse functions.

Experimental Section

Protein Construct Preparation

Yeast Hsp90 dimers (UniProtKB: P02829) supplied with a C-terminal coiled-coil motif (kinesin neck region of *Drosophila melanogaster*) were used to avoid dissociation at low concentrations.[21] Cysteine point mutations allowed specific labeling with donor (D61C) or acceptor (Q385C) fluorophores (see below). Both constructs were cloned into a pET28b vector (Novagen, Merck Biosciences, Billerica, MA). They include an N-terminal His-tag followed by a SUMO-domain for later tag cleavage. The QuikChange Lightning kit (Agilent, Santa Clara, CA) was used to insert an Avitag for specific in vivo biotinylation at the C-terminus of the acceptor construct. *Escherichia coli* BL21star cells (Invitrogen, Carlsbad, CA) were co-transformed with pET28b and pBirAcm (Avidity Nanomedicines, La Jolla, CA) by electroporation (Peqlab, Erlangen, Germany) and expressed according to Avidity's *in vivo* biotinylation protocol. The donor construct was expressed in *E. coli* BL21(DE3)cod+ (Stratagene, San Diego, CA) for 3 h at 37 °C after induction with 1 mM isopropyl β-D-1-thiogalactopyranoside (IPTG) at $OD_{600} = 0.7$ in LB_{Kana}. A cell disruptor (Constant Systems, Daventry, United Kingdom) was used for lysis. Proteins were purified as published[31] (Ni-NTA, tag cleavage, Ni-NTA, anion exchange, size exclusion chromatography). 95% purity was confirmed by SDS-PAGE. Fluorescent labels (Atto550- and Atto647 N-maleimide) were purchased from Atto-tec (Siegen, Germany) and coupled to cysteines according to the supplied protocol. Yeast Aha1 (UniProtKB: Q12449) was fluorescently labeled by replacement of S85 with the unnatural amino acid cyclooctyne-lysine (SCO–L-lysine, Sirius Fine Chemicals SiChem GmbH, Bremen, Germany) and coupling with azide-Atto647 N. Aha1 was a kind gift of Philipp Wortmann. Yeast p23 (Sba1, UniProtKB: P28707) was expressed as S2C mutant and fluorescently labeled with maleimide-Atto647 N. p23 was a kind gift of Johann Thurn. Δ131Δ was expressed as K16C mutant[25] and fluorescently labeled with maleimide-Atto647 N. If not stated differently, all chemicals were purchased from Sigma Aldrich.

Single-Molecule FRET Measurements

smFRET was measured as previously detailed using a home built TIRF setup.[22] Hetero-dimers (acceptor + donor) were obtained by 20 min incubation of 1 μM donor and 0.1 μM biotinylated acceptor homodimers in measurement buffer (40 mM HEPES, 150 mM KCl, and 10 mM $MgCl_2$, pH 7.5) at 47 °C. In this way, predominantly biotinylated heterodimers bind to the polyethylene glycol (PEG, Rapp Polymere, Tuebingen, Germany) passivated and neutravidin (Thermo Fisher Scientific, Waltham, MA) coated fluid chamber. Residual homodimers are recognized using alternating laser excitation (ALEX) of donor and acceptor dyes[32] and excluded from analysis.

All inhibitors were applied at concentrations 100-fold higher than the reported dissociation constant - or the half maximal inhibitory concentration (IC_{50}) if the former was not available. The specific concentrations were 100 μM geldanamycin,[33] 1 μM radicicol,[33] 12 μM PU–H71,[34] 10 μM KU-32.[35] ADP and AMP-PNP were used at 2 mM. To avoid outcompeting of the competitive inhibitors, we excluded additional nucleotides, which would reduce the sensitivity for observing a competitive inhibition effect. In the presence of the C-terminal inhibitor KU32 no nucleotide dependence was observed. Kinetic data analysis was done with the software SMACKS (www.singlemolecule.uni-freiburg.de/SMACKS)

Fluorescence Anisotropy Measurements

Fluorescence anisotropy measurements were performed in measurement buffer. 10 μM Hsp90 with C-terminal zipper (see above) and ±50 μM inhibitor were added to 200 nM labeled Aha1, 400 nM labeled p23 or 400 nM labeled Δ131Δ. Measurements were performed on a Horiba Fluoro-Max 4 fluorescence spectrometer at 25 °C, with excitation at 648 nm (3 nm bandwidth), emission at 660 nm (3 nm bandwidth), 2 s integration time.

Acknowledgements

We thank G. Chiosis and L. M. Neckers for helpful discussions and providing PU–H71. We thank B. S. J. Blagg for providing KU-32. We thank P. Wortmann for Aha1 and J. Thurn for p23. This work was funded by the European Research Council through ERC grant agreement no. 681891 and by the German Science Foundation (SFB863, A4).

Conflict of Interest

The authors declare no conflict of interest.

Keywords: chaperone Hsp90 · FRET · inhibitor · protein conformational dynamics · single molecule

[1] M. Taipale, D. F. Jarosz, S. Lindquist, *Nat. Rev. Mol. Cell Biol.* **2010**, *11*, 515–528.
[2] B. S. J. Blagg, T. D. Kerr, *Med. Res. Rev.* **2006**, *26*, 310–338.
[3] a) M. A. Biamonte, R. van de Water, J. W. Arndt, R. H. Scannevin, D. Perret, W.-C. Lee, *J. Med. Chem.* **2010**, *53*, 3–17; b) L. Neckers, P. Workman, *Clin. Cancer Res.* **2012**, *18*, 64–76; c) K. Sidera, E. Patsavoudi, *Recent Pat. Anti-Cancer Drug Discovery* **2014**, *9*, 1–20; d) T. Taldone, H. J. Patel, A. Bolaender, M. R. Patel, G. Chiosis, *Expert Opin. Ther. Pat.* **2014**, *24*, 501–518; e) A. D. Zuehlke, M. A. Moses, L. Neckers, *Philos. Trans. R. Soc. London Ser. B* **2018**, *373*;
[4] R. Dutta, M. Inouye, *Trends Biochem. Sci.* **2000**, *25*, 24–28.
[5] C. DeBoer, P. A. Meulman, R. J. Wnuk, D. H. Peterson, *J. Antibiot.* **1970**, *23*, 442–447.
[6] P. Delmotte, J. Delmotte-Plaquee, *Nature* **1953**, *171*, 344.
[7] A. Khandelwal, V. M. Crowley, B. S. J. Blagg, *Med. Res. Rev.* **2016**, *36*, 92–118.
[8] R. M. Immormino, Y. Kang, G. Chiosis, D. T. Gewirth, *J. Med. Chem.* **2006**, *49*, 4953–4960.

[9] a) G. Garg, A. Khandelwal, B. S. J. Blagg in *Adv. Cancer Res.* (Eds.: J. Isaacs, L. Whitesell), Academic Press, **2016**; b) M. G. Marcu, A. Chadli, I. Bouhouche, M. Catelli, L. M. Neckers, *J. Biol. Chem.* **2000**, *275*, 37181–37186;
[10] R. L. Matts, A. Dixit, L. B. Peterson, L. Sun, S. Voruganti, P. Kalyanaraman, S. D. Hartson, G. M. Verkhivker, B. S. J. Blagg, *ACS Chem. Biol.* **2011**, *0*.
[11] M. Anyika, M. McMullen, L. K. Forsberg, R. T. Dobrowsky, B. S. J. Blagg, *ACS Med. Chem. Lett.* **2016**, *7*, 67–71.
[12] G. Chiosis, M. N. Timaul, B. Lucas, P. N. Munster, F. F. Zheng, L. Sepp-Lorenzino, N. Rosen, *Chem. Biol.* **2001**, *8*, 289–299.
[13] M. M. U. Ali, S. M. Roe, C. K. Vaughan, P. Meyer, B. Panaretou, P. W. Piper, C. Prodromou, L. H. Pearl, *Nature* **2006**, *440*, 1013–1017.
[14] B. Hellenkamp, P. Wortmann, F. Kandzia, M. Zacharias, T. Hugel, *Nat. Methods* **2017**, *14*, 174–180.
[15] D. R. Southworth, D. A. Agard, *Mol. Cell* **2008**, *32*, 631–640.
[16] C. Prodromou, *BBA-Mol. Cell Res.* **2012**, *1823*, 614–623.
[17] S. Sattin, J. Tao, G. Vettoretti, E. Moroni, M. Pennati, A. Lopergolo, L. Morelli, A. Bugatti, A. Zuehlke, M. Moses et al., *Chem. Eur. J.* **2015**, *21*, 13598–13608.
[18] F. H. Schopf, M. M. Biebl, J. Buchner, *Nat. Rev. Mol. Cell Biol.* **2017**, *18*, 345–360.
[19] T. Weikl, P. Muschler, K. Richter, T. Veit, J. Reinstein, J. Buchner, *J. Mol. Biol.* **2000**, *303*, 583–592.
[20] T. Ha, *Methods* **2001**, *25*, 78–86.
[21] M. Mickler, M. Hessling, C. Ratzke, J. Buchner, T. Hugel, *Nat. Struct. Mol. Biol.* **2009**, *16*, 281–286.
[22] S. Schmid, M. Götz, T. Hugel, *Biophys. J.* **2016**, *111*, 1375–1384.
[23] S. H. McLaughlin, F. Sobott, Z.-p. Yao, W. Zhang, P. R. Nielsen, J. G. Grossmann, E. D. Laue, C. V. Robinson, S. E. Jackson, *J. Mol. Biol.* **2006**, *356*, 746–758.
[24] J. Li, K. Richter, J. Reinstein, J. Buchner, *Nat. Struct. Mol. Biol.* **2013**, *20*, 326 EP -.
[25] T. O. Street, L. A. Lavery, D. A. Agard, *Mol. Cell* **2011**, *42*, 96–105.
[26] A. Rodina, M. Vilenchik, K. Moulick, J. Aguirre, J. Kim, A. Chiang, J. Litz, C. C. Clement, Y. Kang, Y. She et al., *Nat. Chem. Biol.* **2007**, *3*, 498–507.
[27] A. Röhl, J. Rohrberg, J. Buchner, *Trends Biochem. Sci.* **2013**, *38*, 253–262.
[28] a) C. Prodromou, *J. Biochem.* **2016**, *473*, 2439–2452; b) B. K. Zierer, M. Rubbelke, F. Tippel, T. Madl, F. H. Schopf, D. A. Rutz, K. Richter, M. Sattler, J. Buchner, *Nat. Struct. Mol. Biol.* **2016**, *23*, 1020–1028.
[29] M. G. Marcu, T. W. Schulte, L. Neckers, *JNCI J. Natl. Cancer Inst.* **2000**, *92*, 242–248.
[30] B.-G. Yun, W. Huang, N. Leach, S. D. Hartson, R. L. Matts, *Biochemistry* **2004**, *43*, 8217–8229.
[31] M. Jahn, A. Rehn, B. Pelz, B. Hellenkamp, K. Richter, M. Rief, J. Buchner, T. Hugel, *Proc. Natl. Acad. Sci. USA* **2014**, *111*, 17881–17886.
[32] N. K. Lee, A. N. Kapanidis, Y. Wang, X. Michalet, J. Mukhopadhyay, R. H. Ebright, S. Weiss, *Biophys. J.* **2005**, *88*, 2939–2953.
[33] S. M. Roe, C. Prodromou, R. O'Brien, J. E. Ladbury, P. W. Piper, L. H. Pearl, *J. Med. Chem.* **1999**, *42*, 260–266.
[34] H. He, D. Zatorska, J. Kim, J. Aguirre, L. Llauger, Y. She, N. Wu, R. M. Immormino, D. T. Gewirth, G. Chiosis, *J. Med. Chem.* **2006**, *49*, 381–390.
[35] Y. Lu, S. Ansar, M. L. Michaelis, B. S. J. Blagg, *Bioorg. Med. Chem.* **2009**, *17*, 1709–1715.

Manuscript received: April 15, 2018
Accepted Article published: April 20, 2018
Version of record online: May 25, 2018